Cellular/Molecular

Perisynaptic Localization of δ Subunit-Containing GABA$_A$ Receptors and Their Activation by GABA Spillover in the Mouse Dentate Gyrus

Weizheng Wei,[1,3] **Nianhui Zhang,**[2,3] **Zechun Peng,**[2,3] **Carolyn R. Houser,**[2,3,4] **and Istvan Mody**[1,3]

Departments of [1]Neurology and Physiology and [2]Neurobiology, and [3]Brain Research Institute, The David Geffen School of Medicine at University of California Los Angeles, Los Angeles, California 90095, and [4]Research Service, Department of Veterans Affairs Greater Los Angeles Healthcare System, West Los Angeles, Los Angeles, California 90073

In cerebellar granule cells, δ subunit-containing GABA$_A$ receptors are found exclusively at extrasynaptic sites, but their subcellular distribution in other brain areas is poorly understood. We examined the anatomical localization and physiological activation of these receptors in adult mouse dentate gyrus granule cells. Immunocytochemistry revealed a high density of δ subunits in the molecular layer and a much lower density in the cell body layer. At the ultrastructural level, immunogold-labeled δ subunits were found at the edge of symmetric synapses on granule cell dendrites. Functional correlates of this perisynaptic localization were obtained by comparing inhibitory responses in δ subunit-deficient (δ−/−) and wild-type (wt) mice. In whole-cell recordings at 22°C, the weighted decay time constants (τ_w) of spontaneous IPSCs (sIPSCs) were significantly longer in wt mice but were similar at 34°C, reflecting the role of temperature-dependent GABA uptake in shaping sIPSC decay. IPSCs evoked by minimal stimulation (eIPSCs) near the somata had similar τ_w in δ−/− and wt mice, but eIPSCs elicited from dendritic sites decayed significantly more slowly in wt mice, consistent with a higher density of δ subunit-containing receptors in the molecular layer. The τ_w of dendritic eIPSCs of wt mice were shortened by ZnCl$_2$ (10 μM), reflecting the high Zn^{2+} sensitivity of δ subunit-containing GABA$_A$ receptors, and were prolonged by the GAT-1 GABA transporter inhibitor NO711 (10 μM). Our results demonstrate a perisynaptic localization of δ subunit-containing GABA$_A$ receptors and indicate that these receptors can be activated by GABA overspill in the molecular layer.

Key words: hippocampus; IPSCs; immunocytochemistry; GABA uptake; postembedding immunogold; zinc

Introduction

GABA$_A$ receptors composed of heteropentameric subunits show a considerable diversity, but individual subunits exhibit specific expression patterns in certain brain regions, and a distinct subcellular localization of the subunits can be found even within a given nerve cell (McKernan and Whiting, 1996; Korpi et al., 2002a). The δ subunit is one of the GABA$_A$ receptor subunits with a highly specific regional and subcellular distribution. It is abundant in cerebellar and dentate gyrus granule cells, some cortical areas, thalamic relay nuclei, and the striatum (Wisden et al., 1992; Fritschy and Möhler, 1995; Sperk et al., 1997; Pirker et al., 2000; Peng et al., 2002). This subunit forms a specific partnership with the α6 subunit in the cerebellum (Jones et al., 1997) and with the α4 subunit in the rest of the forebrain (Sur et al., 1999; Korpi et

al., 2002b). At the ultrastructural level in cerebellar granule cells, receptors formed by this subunit appear to be confined specifically to extrasynaptic areas (Nusser et al., 1998b), a few micrometers away from inhibitory synapses. In these cells, the α6δ subunit-containing receptors are thought to underlie a tonic form of inhibition (Brickley et al., 2001) capable of controlling the action potential firing (Brickley et al., 1996) and synaptic activation of granule cells (Hamann et al., 2002). Its extrasynaptic localization (Nusser et al., 1998b), high GABA affinity, and marginal desensitization (Saxena and Macdonald, 1994, 1996; Wohlfarth et al., 2002) make this receptor ideal for being activated by ambient levels of GABA found in the extracellular space (Mody, 2001).

Consistent with an important role of δ subunit-containing GABA$_A$ receptors in the regulation of neuronal excitability, δ−/− mice have epilepsy, are less sensitive to anesthetic steroids, and show other signs of hyperexcitability (Mihalek et al., 1999; Spigelman et al., 2002) despite the compensatory upregulation of other GABA$_A$ receptor subunits. In contrast to several descriptions of δ subunit localizations at the light microscopic level in the rodent brain (Fritschy and Möhler, 1995; Sperk et al., 1997; Pirker et al., 2000; Peng et al., 2002), there is little information about the subcellular distribution of δ subunits outside the cerebellum. Moreover, the direct assessment of the δ subunit-

containing GABA$_A$ receptors in shaping inhibitory neuronal signaling is unclear. We have shown previously that the insensitivity to benzodiazepine (BZ) of the tonic GABA$_A$ receptor-mediated conductance in rat dentate gyrus granule cells is consistent with δ subunit-containing receptors underlying this conductance (Nusser and Mody, 2002). Moreover, some changes in the kinetics of spontaneous and miniature IPSCs were described in δ null-mutant mice (Spigelman et al., 2002). The purpose of the present study was to examine the cellular and subcellular localization of δ subunit-containing GABA$_A$ receptors in the dentate gyrus and to examine their activation during spontaneous and evoked GABA release. Our findings indicate that these receptors are mainly localized perisynaptically on the dendrites of dentate gyrus granule cells and are activated by GABA spillover from the synaptic cleft.

Some of our findings have been published previously in abstract form (Wei et al., 2002).

Materials and Methods

Animals. Targeted disruption of the δ subunit gene of the GABA$_A$ receptor in mouse embryonic stem cells and production of homozygous null (δ−/−) and wild-type (δ+/+) mice have been described in detail previously (Mihalek et al., 1999). These mice were of a C57BL/6J × strain 129Sv/SvJ genetic background, and all δ−/− and δ+/+ mice were produced from heterozygous mating pairs. The mice required no special care but may have had latent epileptiform activity noticeable only in EEG recordings (Mihalek et al., 1999). Normal C57BL/6J mice (Harlan Sprague Dawley, Indianapolis, IN) were also used in the immunohistochemical studies. All mice were 30–60 d of age. All animal-use protocols conformed to National Institutes of Health guidelines and were approved by the University of California Los Angeles Chancellor's Animal Research Committee.

Antisera. Subunit-specific antisera that recognize the δ and α2 subunits of the GABA$_A$ receptor were used in comparative immunohistochemical studies. The δ antiserum was produced in rabbits to a synthetic peptide sequence, δ(1–44), and was kindly provided by W. Sieghart (University of Vienna, Vienna, Austria). The specificity of the antiserum has been demonstrated previously in immunochemical (Jechlinger et al., 1998) and immunohistochemical (Fritschy and Möhler, 1995; Sperk et al., 1997) studies. No specific labeling was evident in δ subunit-deficient mice, and this further supports the specificity of the antiserum (Peng et al., 2002).

Antiserum to the α2 subunit was produced in guinea pig to a synthetic peptide sequence, α2(1–9), and was generously provided by J.-M. Fritschy (University of Zurich, Zurich, Switzerland). The specificity of the antiserum has been demonstrated previously (Marksitzer et al., 1993; Fritschy and Möhler, 1995).

Tissue preparation for microscopy. Mice were deeply anesthetized with sodium pentobarbital (90 mg/kg, i.p.) and perfused through the ascending aorta with a fixative solution of 4% paraformaldehyde in phosphate buffer, pH 7.3, for light microscopy or with the same fixative with the addition of 0.1% glutaraldehyde for electron microscopy. The brains were kept *in situ* at 4°C for 1–2 hr, removed from the skull, postfixed in the same fixative as that used for perfusion for an additional 1 hr (light microscopy) or 2–4 hr (electron microscopy), and then rinsed thoroughly in buffer.

Immunohistochemistry for light microscopy. Forebrain blocks that included the hippocampal formation were cryoprotected in a 30% sucrose solution, frozen, and sectioned coronally at 30 μm with a cryostat. The tissue was processed for immunohistochemical localization of the δ and α2 subunits with methods described previously by Peng et al. (2002).

Before immunohistochemical processing, sections were incubated in 1% H$_2$O$_2$ for 30 min to reduce endogenous peroxidase-like activity. After a rinse in 0.1 M Tris-buffered saline (TBS), pH 7.3, the sections were processed with water bath antigen-retrieval methods (Jiao et al., 1999; Peng et al., 2002). Free-floating sections were incubated in 0.05 M sodium citrate solution, pH 8.6, for 30 min at room temperature (RT) and then

heated in a water bath in the same solution at 90°C for 70 min. The sections were allowed to cool at RT for 30 min and then rinsed in TBS.

Sections were processed for immunohistochemistry with avidin–biotin–peroxidase methods (Vectastain Elite ABC; Vector Laboratories, Burlingame, CA). Sections were incubated in 10% normal goat serum (NGS) in TBS containing 0.3% Triton X-100 and avidin (200 μl/ml) for 3–4 hr to reduce nonspecific binding. The sections were incubated with primary antiserum (anti-δ, 1:3000; anti-α2, 1:10,000) diluted in TBS containing 2% NGS and biotin (200 μl/ml) overnight at RT. After rinsing, the sections were incubated in appropriate secondary antisera (biotinylated goat anti-rabbit IgG or biotinylated goat anti-guinea pig IgG) diluted 1:1000 in 0.1 M TBS, pH 7.3, containing 2% NGS for 1 hr. After a thorough rinse, the sections were incubated in avidin–biotin–peroxidase complex (1:200 in 0.075 M phosphate buffer, pH 7.3) for 1 hr. To reveal the peroxidase labeling, some sections were processed with 0.06% diaminobenzidene tetrahydrochloride (DAB) and 0.006% H$_2$O$_2$ diluted in PBS for 10–15 min, and immunolabeling was enhanced by incubation in 0.003% osmium tetroxide in PBS for 30 sec. Other sections were processed with a glucose oxidase–DAB–nickel method (Shu et al., 1988). After rinsing, sections were mounted on gelatin-coated slides, dehydrated, and coverslipped. Control sections were processed with either omission of the primary antiserum or substitution of the primary antisera with appropriate normal serum. No specific immunolabeling was observed with these conditions.

Immunolabeling for electron microscopy. Forebrain tissue was sectioned coronally at 0.5–1 mm with a razor blade, and small blocks of tissue that contained the molecular and granule cell layers were trimmed from the upper blade of the dentate gyrus. These specimens were immersed in 5% sucrose in phosphate buffer (0.1 M), pH 7.4, and then in 10, 20, and 30% glycerol in phosphate buffer for 2 hr each.

Methods for freeze substitution and low-temperature embedding were on the basis of those of Matsubara et al. (1996). Cryoprotected sections were rapidly plunged into liquid propane cooled by liquid nitrogen to −190°C in a cryofixation unit (EM CPC; Leica, Wien, Austria). Tissues were then transferred to a cryosubstitution unit (EM AFS; Leica) that was programmed for all subsequent steps. Specimens were immersed in 4% uranyl acetate (Electron Microscopy Sciences, Fort Washington, PA) dissolved in anhydrous methanol for 24 hr at −90°C, and the temperature was then raised to −45°C by steps of 5°C. The specimens were rinsed in methanol and infiltrated with Lowicryl HM20 resin (Electron Microscopy Sciences) for 48 hr at −45°C. The resin was polymerized with ultraviolet light (360 nm) for 24 hr at −45°C, and the temperature was then increased progressively by steps of 4°C until it reached 0°C.

In preparation for postembedding immunogold labeling, ultrathin sections were cut on a microtome (Reichert-Jung, Vienna, Austria), picked up on nickel mesh grids that were freshly coated with a Coat-Quick "G" pen (Electron Microscopy Sciences), and air dried at RT. The tissue was processed with slight modifications of the immunogold labeling methods of Matsubara et al. (1996). All incubations were performed under humid conditions in a culture dish. Ultrathin sections were treated with either a saturated solution of sodium hydroxide in 100% ethanol for 2–3 sec or 0.2% sodium hydroxide in distilled water for 5 min and then with 0.1% sodium borohydride in 0.01 M TBS, pH 7.4, for 10 min. After rinsing, ultrathin sections were incubated in 2% human serum albumin (HAS) (Sigma, St. Louis, MO) in TBS containing 0.1% Triton X-100 for 10 min and in the same solution with the addition of 0.05 M glycine for 7 min. Sections were incubated in 2% HSA in TBS for 1.5 hr to reduce nonspecific binding and then incubated in the primary antiserum, rabbit anti-δ subunit (1:100) or guinea pig anti-α2 subunit (1:1000), in TBS containing 2% HSA for 18–24 hr at RT. After a rinse with 0.05 M Tris-HCl buffer containing polyethylene glycol (50 mg/ml), sections were incubated for 2.5 hr in an appropriate secondary antisera conjugated to 10 nm colloidal gold particles, diluted 1:20 in Tris-HCl buffer (0.05 M), pH 8.0, containing 2% HSA. The secondary antisera were (1) either goat anti-rabbit IgG fragments, F(ab')$_2$ (British BioCell International; distributed by Ted Pella, Inc., Redding, CA) or goat anti-rabbit IgG(H+L) (Amersham Biosciences, Piscataway, NJ) and (2) goat anti-guinea pig IgG (Aurion; distributed by Electron Microscopy Sciences). Sections

were then rinsed thoroughly and stained with a saturated solution of uranyl acetate for 40 min and lead citrate for 4 min. The sections were studied and photographed with a Zeiss C10 or JEOL 100CX II electron microscope.

After initial studies of the subcellular localization of the δ subunit of the GABA_A receptor, the immunolabeling on granule cell dendrites was analyzed in greater detail. Randomly selected series of δ subunit-labeled synaptic profiles within the molecular layer were photographed at a primary magnification of 19,000× and a final print magnification of 49,500×. The distribution of δ subunit labeling at or near symmetric synapses on granule cell dendrites was determined. Symmetric synaptic contacts were operationally defined as regions with close apposition between an axon terminal and a putative granule cell dendrite at which the presynaptic and postsynaptic membranes were precisely parallel. Such contacts generally included a thin postsynaptic density and some electron-dense material in the cleft between the membranes. The ends of the synaptic contacts were defined as the sites at which the presynaptic and postsynaptic membranes were no longer strictly parallel and the postsynaptic density was no longer evident. The location of colloidal gold particles was determined for each symmetric synapse that exhibited immunogold labeling on the postsynaptic structure. The location of gold particles along the membranes was classified as (1) within the central third of the synaptic contact only, (2) within both the central and outer third(s) of the synaptic contact, (3) directly at the end(s) of the synaptic contact or within 30 nm of the ends of the contact (perisynaptic), or (4) outside the synaptic contact but along the adjacent dendritic membrane at a distance >30 nm from the end of the contact (extrasynaptic).

To provide a comparison with the δ subunit localization, the location of the α2 subunit of the GABA_A receptor was also studied in the molecular layer of the dentate gyrus. Nonoverlapping, randomly selected fields of α2-labeled sections were photographed, and the α2 labeling was classified according to the criteria described above for the δ subunit labeling.

Electrophysiological recordings. Transverse mouse hippocampal slices were prepared as described previously (Stell and Mody, 2002). Briefly, mice were anesthetized individually with halothane before decapitation. The brains were then removed and placed into an ice-cold artificial CSF (ACSF) containing (in mM): 126 NaCl, 2.5 KCl, 2 CaCl_2, 2 MgCl_2, 1.25 NaH_2PO_4, 26 NaHCO_3, 10 D-glucose, pH 7.3, when bubbled with 95% O_2 and 5% CO_2. Horizontal 350-μm-thick brain slices were cut with a Vibratome (Leica VT1000S) and stored at 32°C or room temperature (24°C) for >1 hr until they were transferred to the recording chamber, in which the slices were perfused continuously at 3 ml/min with 33–34°C or 24°C ACSF containing 3 mM kynurenic acid (Sigma) saturated with 95% O_2 and 5% CO_2.

All somatic whole-cell recordings were made in the dentate gyrus granule cell layer of visually identified neurons (custom-made infrared differential interference contrast videomicroscopy; 40× water immersion objective) with an Axopatch 200A amplifier (Axon Instruments, Foster City, CA). Recording electrodes were pulled from borosilicate glass capillaries with an inner filament (KG-33, 1.12 mm inner diameter, 1.5 mm outer diameter; Garner Glass) pulled to tip diameters of ~1.0 μm in two stages using a vertical puller (Narishige PP-83). Intracellular solutions contained the following (in mM): 128 CsCl, 10 HEPES, 10 EGTA, 5 MgATP, and 5 QX-314, adjusted to pH 7.25 with CsOH (280– 290 mOsm). Voltage-clamp recordings were made at $V_h = -70$ mV. The DC resistances of the electrodes were 4–6 MΩ. Series resistance was compensated by 70–90% using lag values of 7–10 μsec. Before compensation, series resistance was <15 MΩ. For the minimal stimulation experiments, the extracellular Ca^{2+}/Mg^{2+} ratio was changed to 1:2 (1.5 mM CaCl_2 and 3 mM MgCl_2). Two stimulating electrodes made of Θ glass pipettes (1.5 mm outside Ø, pulled to a tip Ø of 1 μm) and filled with 1 M NaCl were placed as follows: one was positioned near the recorded granule cell soma (5~10 μm away), and the other was positioned in the molecular layer. The two stimulating electrodes were used to elicit evoked IPSCs (eIPSCs) by alternately delivering stimuli to the two sites at 0.1 Hz. The constant current minimal stimuli had pulse widths of 20–40 μsec triggered from a digital stimulator (Neuro Data PG4000).

All recordings were acquired and low-pass filtered (eight-pole Bessel; Brownlee Precision 200) at 3 kHz and digitized on-line at 20 kHz using a
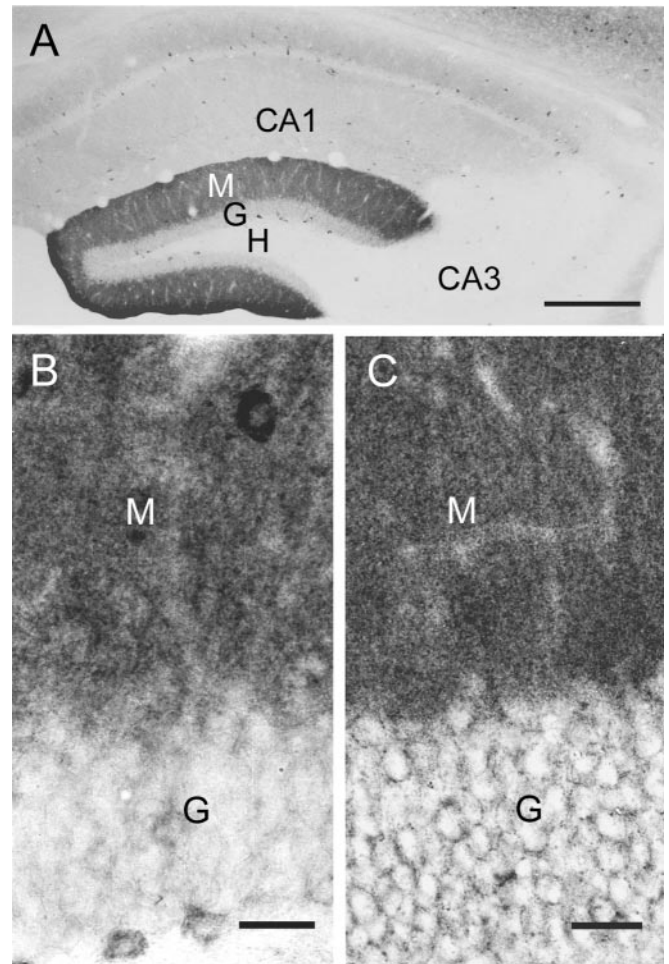
Figure 1. Distribution of δ and α2 subunits at the light microscopic level. *A*, Moderate diffuse immunolabeling of the δ subunit is found in the molecular layer (M) of the dentate gyrus, and only light labeling is evident in the granule cell layer (G). Light diffuse labeling is present in the dendritic layers of CA1, but very little labeling is detected in CA3 and the hilus (H). Moderate to lightly labeled interneurons are present throughout the hippocampus. *B, C,* Immunoreactivity for both δ (*B*) and α2 (*C*) subunits is relatively strong in the molecular layer (M) of the dentate gyrus. In the granule cell layer (G), labeling of the δ subunits is low around the cell bodies of the granule cells (*B*). This contrasts with much stronger labeling of the α2 subunit in the granule cell layer, where the labeling outlines the contours of many granule cell somata (*C*). In *B*, several putative interneurons in the granule cell and molecular layers are moderately labeled for the δ subunit. Scale bars: *A*, 300 μm; *B, C*, 25 μm.

PCI-MIO-IGE data acquisition board (National Instruments, Austin, TX). Data were acquired and analyzed using our custom-written software. The IPSCs were detected and analyzed as described previously (Nusser et al., 2001). Paired and unpaired *t* test analyses were performed by Origin 7.0 software. The group data are expressed as mean ± SEM, with *n* indicating the number of recorded cells. The means are significantly different if $p < 0.05$.

## Results

Enrichment of δ subunit-containing GABA_A receptors in the molecular layer of the dentate gyrus

Within the hippocampal formation, δ subunit-immunoreactivity (IR) was highly concentrated in the molecular layer of the dentate gyrus (Fig. 1*A*). Much lower levels of δ subunit labeling were present in dendritic regions of CA1 (stratum radiatum and stratum oriens), and very little labeling was evident in CA3 (Fig. 1*A*).

In the dentate gyrus, high levels of δ subunit-IR in the molecular layer contrasted with low levels of labeling within the granule
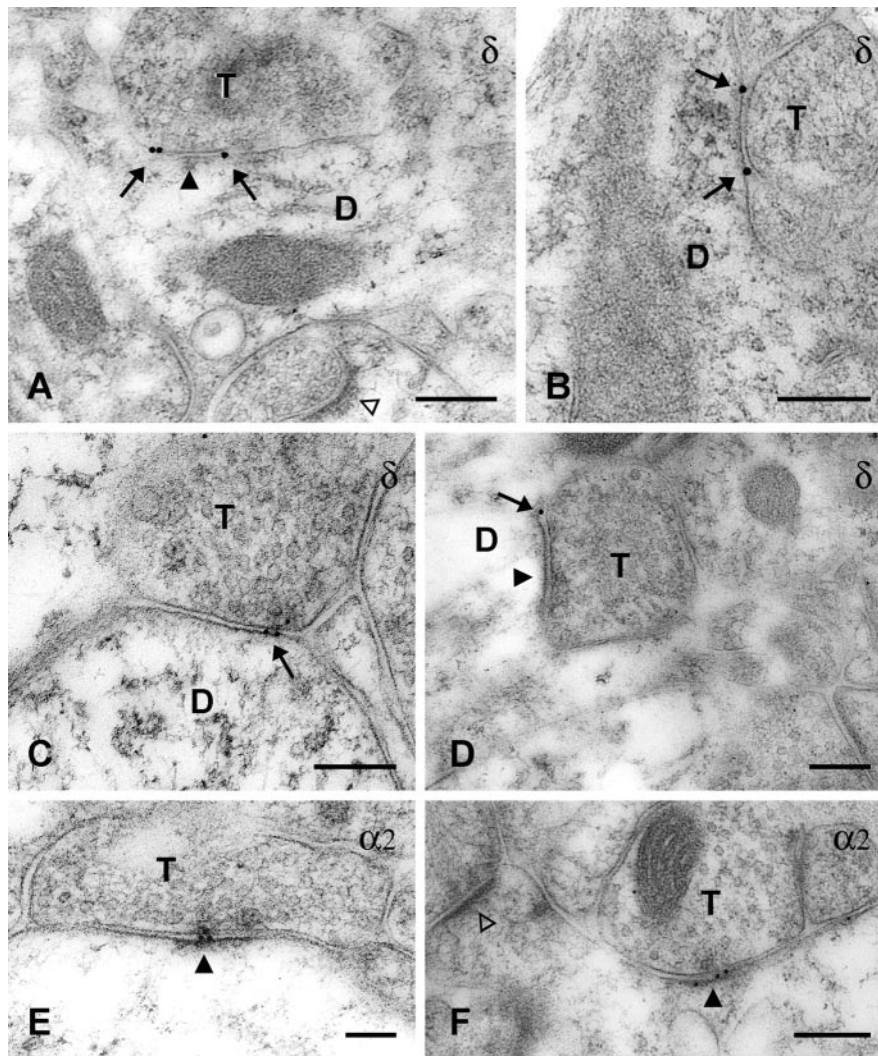
Figure 2. Immunogold labeling of the δ and α2 subunits of the GABA_A receptor. Gold particles that indicate the location of the δ subunit (A–D, arrows) were present on or near the plasma membrane of dendrites (D) that were in contact with axon terminals (T). Gold particles were localized primarily at perisynaptic sites, just outside or at the outer edge of symmetric synapses (A, D, solid arrowheads). In contrast, immunogold labeling for the α2 subunit was observed directly at symmetric synapses (E, F, solid arrowheads). No labeling for either the δ or α2 subunit was observed at asymmetric synapses on spines (A, F, open arrowheads). Scale bars, 0.2 μm.

Perisynaptic localization of δ subunit-containing GABA_A receptors

In δ subunit-labeled specimens, colloidal gold particles were frequently located on or very near the plasma membrane of dendrites in the molecular layer (Fig. 2A–D), thus indicating localization of the δ subunit primarily on the surface of the postsynaptic structures. Colloidal gold particles were located predominantly near the ends or outer regions of symmetric synapses of putative dentate granule cell dendrites (Fig. 2A–D). At some synapses, gold particles were present at both ends of the synaptic junction (Fig. 2A,B), whereas at others, labeling was detected at only one end of the synaptic contact (Fig. 2C,D). Further analysis of δ subunit localization was conducted in a series of randomly selected synapses that exhibited δ subunit labeling in the molecular layer (n = 40). In this sample, no synapses exhibited δ subunit labeling near the center of the synaptic contact. Labeling was evident either at or near the ends of the synaptic contact in 90% (n = 36) of the labeled synapses. At these synapses, δ subunit labeling was located precisely to the ends of the synaptic contacts (Fig. 2A,B,D), within the outer 30 nm of the synaptic contact (Fig. 2C), or immediately outside the synaptic contact but within 30 nm of the end of the synapse. The δ subunit localization at all of these synapses was considered perisynaptic because of the close proximity of the gold particles to the ends of the synaptic contacts. In a subset of these synapses, colloidal gold particles extended beyond the perisynaptic site into either the outer third of the synaptic contact (n = 2) or the extrasynaptic region (n = 3). In the 10% (n = 4) of synaptic profiles that did not exhibit perisynaptic labeling, colloidal gold particles were present within either the outer third of the synapse (n = 2) or at a distance of 30–100 nm from the end of the synapse (n = 2). The latter labeling, although in relatively close proximity to the synapse, was classified as extrasynaptic in this analysis. Thus δ subunit labeling was found primarily at the periphery of symmetric synapses, in a perisynaptic location, in a very high percentage of the analyzed synapses.

Immunogold labeling of the α2 subunit was conducted to compare the localization of the δ and α2 subunits in tissue from the same animals that had been processed with similar immunogold labeling methods. In contrast to the localization of the δ subunit, the α2 subunit was frequently located directly at synaptic junctions and often near the center of the synaptic profile (Fig. 2E,F). Such synaptic localization of the α2 subunit is consistent with previous descriptions of the ultrastructural location of this subunit (Nusser et al., 1996). In an analysis of all α2-labeled symmetric synapses (n = 40) within randomly selected fields from the dentate molecular layer, 65% (n = 26) exhibited α2 labeling within the central third of the synaptic contact only, and

cell layer (Fig. 1A,B). Only limited labeling was evident around the somata of most granule cells (Fig. 1B). Moderate labeling, however, was present within the cell bodies of some putative interneurons within the granule cell and molecular layers (Fig. 1B).

To verify that the low levels of δ subunit-IR in the granule cell layer did not result from methodological factors, adjacent sections were processed for localization of the α2 subunit of the GABA_A receptor, a subunit that has been localized previously within the granule cell layer (Fritschy and Möhler, 1995; Sperk et al., 1997) and at axosomatic synapses on pyramidal cells (Nusser et al., 1996). With immunohistochemical methods that were essentially identical to those used for localization of the δ subunit, substantial α2 labeling was evident around granule cell somata (Fig. 1C). Thus, although labeling for both subunits was high in the molecular layer of the dentate gyrus, labeling for the δ subunit was substantially lower than that for the α2 subunit in the granule cell layer (Fig. 1, compare B, C).

Table 1. Properties of sIPSCs recorded at 34°C in dentate gyrus granule cells of wt and δ−/− mice

	wt	δ−/−
Frequency (Hz)	15.0 ± 1.7	13.6 ± 2.1
Amplitude (pA) @V_h = −70 mV	−52.4 ± 5.4	−48.3 ± 3.3
RT$_{10–90\%}$ (msec)	0.427 ± 0.03	0.396 ± 0.03
τ_w (msec)	4.29 ± 0.24	4.58 ± 0.27
Number of cells	15	16

The data are pooled from several experiments.

32.5% (n = 13) showed labeling within both the central and outer thirds of the contact. Thus in 97.5% of the labeled synapses, the α2 labeling was present directly at the synaptic contact. In this sample, no synapse exhibited α2 labeling exclusively at the ends of the synaptic contacts, but one synapse displayed labeling at a distance of 30–100 nm beyond the end of the synapse. Thus, in the dentate molecular layer, the central synaptic localization of the α2 subunit contrasted sharply with the perisynaptic location of the δ subunit.

Immunogold labeling for the δ subunit was not detected at axosomatic synapses on dentate granule cells; however, low levels of δ subunit labeling were present in the granule cell layer in the light microscopic sections. This suggests that levels of the δ subunit on granule cell somata may have been too low to be detected with the present immunogold labeling methods.

Characteristics of sIPSCs in dentate gyrus granule cells of wt and δ−/− mice

Considering the anatomical findings revealing the perisynaptic location of δ subunit-containing receptors, we wanted to know whether these receptors were activated by spontaneously released transmitter. We recorded sIPSCs in the whole-cell patch-clamp configuration at 34°C in wt and δ−/− mice. The frequencies, amplitudes, 10–90% rise times, and τ_w of sIPSCs were not significantly different between the two preparations, as shown by the pooled data from all experiments (Table 1). This finding indicates either that in wt animals δ subunit-containing GABA$_A$ receptors were not activated during sIPSCs or that in δ−/− granule cells the missing δ subunits have been replaced with other subunits that conferred highly similar kinetic characteristics to the receptors.

sIPSC conductance and voltage dependence of decay

The amplitude of miniature IPSCs (mIPSCs) recorded at a given voltage was reported not to be altered in δ−/− dentate gyrus granule cells (Mihalek et al., 1999) or in thalamic neurons (Porcello et al., 2003). Nevertheless, we wanted to examine the conductance of synaptic receptors underlying sIPSCs, because δ subunit-containing GABA$_A$ receptors may have a slightly smaller single-channel conductance than their γ2 subunit-containing counterparts (Haas and Macdonald, 1999). There is a bias introduced in estimating the amplitude of the events at different holding potentials when changes in the driving force for the permeant ion (Cl$^-$) drive events into the baseline noise, thus resulting in apparent reductions in frequency (Stell and Mody, 2002). To obtain the real sIPSC conductance, we have used the largest amplitude matching technique (Stell and Mody, 2002). Briefly, reference events were considered to be those recorded closest to the Cl$^-$ reversal potential (0 mV), i.e., at −20 and +20 mV, respectively. At the other positive or negative holding potentials (−40, −70, and +40 mV), only the largest events were considered for the analysis corresponding in number to those recorded at −20
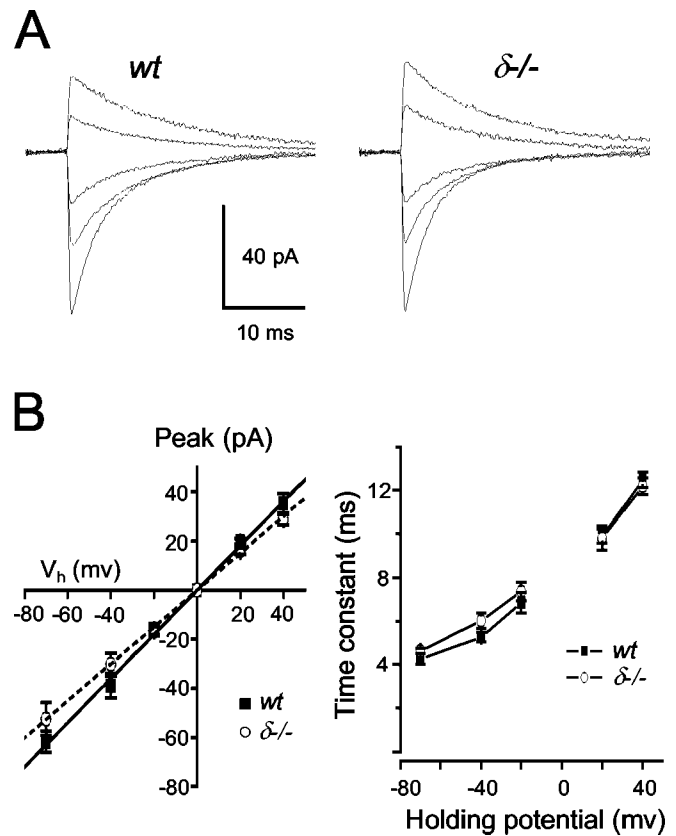
Figure 3. sIPSC conductance and voltage dependence of τ_w in wt and δ−/− granule cells. *A,* Each trace is the average of >100 sIPSCs recorded at five different holding potentials of −70, −40, −20, +20, and +40 mV, respectively. *B,* Left panel, The sIPSC conductance was calculated from linear fits to the peak amplitude versus holding potential plots. The average peak amplitudes were obtained by the method of highest amplitude count matching (for details, see Results) to avoid the bias introduced by losing events to the noise when the holding potential was closer to E$_{Cl}$. There was no significant difference between the slope conductances of sIPSCs recorded in the two genotypes (0.90 ± 0.04 pS in wt vs 0.78 ± 0.05 pS in δ−/−). Right panel, The voltage dependence of τ_w was also comparable between wt and δ−/− granule cells. The number of cells is n = 10 for wt and n = 9 for the δ−/−.

and +20, respectively, during the same collection period. This technique assumes that the frequency of the events remains constant at various holding potentials. This may not be the case if a depolarization-induced suppression of inhibition (DSI) mediated by the presynaptic activation of cannabinoid receptors (Wilson and Nicoll, 2001) is activated during the depolarization. In sharp contrast to hippocampal pyramidal cells (Pitler and Alger, 1994), however, and for reasons that remain to be determined, we were unable to record any DSI in dentate gyrus granule cells (V. Riazanski and I. Mody, unpublished observations), thus eliminating the possibility of an altered sIPSC frequency at depolarized potentials. The slope conductance of the sIPSCs calculated using the largest amplitude event count matching (Stell and Mody, 2002) was not significantly different between wt (0.90 ± 0.04 nS) and δ−/− granule cells (0.78 ± 0.05 nS) (Fig. 3*A,B*).

In several central neurons, including granule cells of the dentate gyrus, there is a voltage-dependent prolongation of mIPSC decay (Otis and Mody, 1992). This has been attributed to voltage-dependent changes in GABA$_A$ receptor gating (Mellor and Randall, 1998) and may be different between γ and δ subunit-containing receptors. We examined the effects of membrane voltage on sIPSC amplitudes and decay kinetics over a wide range of holding potentials at 34°C. Because the membrane was depo-

larized, individual IPSCs decayed with a slower rate. We found no significant differences ($p > 0.05$; Student's t test) in the voltage dependence of sIPSC amplitudes (Fig. 3A) and decay time constants (Fig. 3B) between granule cells of wt ($n = 10$) and δ−/− mice ($n = 9$). This shows that transmembrane voltage does not change the characteristics of GABA_A receptor-mediated sIPSC amplitude and decay shaping.

Temperature-dependent differences in the decay of sIPSCs recorded in wt and δ−/− dentate gyrus granule cells and the effect of Zn^{2+}

Temperature is known to affect the decay kinetics of GABA_A receptor-mediated sIPSCs in dentate gyrus granule cells (Otis and Mody, 1992), and it is possible that receptor combinations with different subunits respond differently to changes in temperature. Temperature also has a significant effect on GABA uptake (Mitchell and Silver, 2000), because the temperature dependence (Q_{10}) of uptake processes is quite high (Wadiche and Kavanaugh, 1998). Our anatomical findings of a perisynaptic localization of δ subunit-containing receptors make it likely for GABA uptake at and around synapses to alter the activation of these receptors by synaptically released GABA. Therefore, we examined the temperature sensitivity of the sIPSC decay in wt and δ−/− mice. At physiological temperatures (34°C), sIPSCs had monoexponential decays in whole-cell voltage-clamp recordings at holding potentials between −60 and −70 mV.

At near physiological temperature (34°C), the decay time constant of sIPSCs in wt (4.10 ± 0.22 msec; $n = 5$) was similar to the average values recorded in δ−/− mice (4.91 ± 0.45 msec; $n = 6$). In contrast, at room temperature (22°C), there was a significant difference between the decay time constants of sIPSCs in wt (17.56 ± 1.15 msec; $n = 10$) and δ−/− mice (13.90 ± 0.58 msec; $n = 9$) ($p < 0.01$; Student's t test) (Fig. 4A,B). In the same cells, we also compared the amplitudes of sIPSCs between wt (at 22°C, 41.79 ± 6.72 pA, $n = 10$; at 34°C, 56.60 ± 3.39 pA, $n = 9$) and δ−/− mice (at 22°C, 38.19 ± 6.66 pA, $n = 9$; at 34°C, 50.76 ± 3.72 pA, $n = 6$) and found no significant differences between the two genotypes ($p > 0.05$; Student's t test) (Fig. 4C).

GABA_A receptors containing δ subunits are generally thought to be more sensitive to Zn^{2+} than those containing γ subunits (Korpi et al., 2002a). If δ subunit-containing receptors are activated by action potential-dependent spillover of GABA only at room temperature when GABA uptake is considerably slowed down (Mitchell and Silver, 2000), the effect of Zn^{2+} on sIPSCs should be more evident at room temperature. We therefore examined the effects of Zn^{2+} at near-physiological and room temperature on the decay of sIPSCs in wt and δ−/− mice. As reported previously in rat granule cells (Buhl et al., 1996; Cohen et al., 2003), Zn^{2+} (10 μM) had no significant effect ($p > 0.05$; paired t test) on the weighted decay time constants of sIPSCs recorded in either wt or δ−/− neurons at 34°C (wt: 5.07 ± 0.32 msec, $n = 5$ in control, and 5.48 ± 0.17 msec, $n = 5$ in 10 μM $ZnCl_2$; δ−/−: 4.01 ± 0.19 msec, $n = 6$ in control, and 4.15 ± 0.22 msec, $n = 6$ in 10 μM $ZnCl_2$) (Fig. 5A). In contrast, perfusion of 10 μM $ZnCl_2$ at 22°C significantly shortened ($p < 0.01$; paired t test) the decay time constants of sIPSCs recorded in wt cells from 18.47 ± 1.11 to 14.90 ± 0.52 msec ($n = 7$) (Fig. 5B). The same treatment had no effect ($p > 0.05$; paired t test) on the decays of sIPSCs recorded in δ−/− granule cells (weighted decay: 14.17 ± 0.23 msec under control conditions, and 13.95 ± 0.36 msec in the presence of 10 μM $ZnCl_2$; $n = 5$) (Fig. 5B). Statistical comparisons also showed that the value of the decay time constant recorded at room temperature in the presence of Zn^{2+} in wt cells (Fig. 5B)
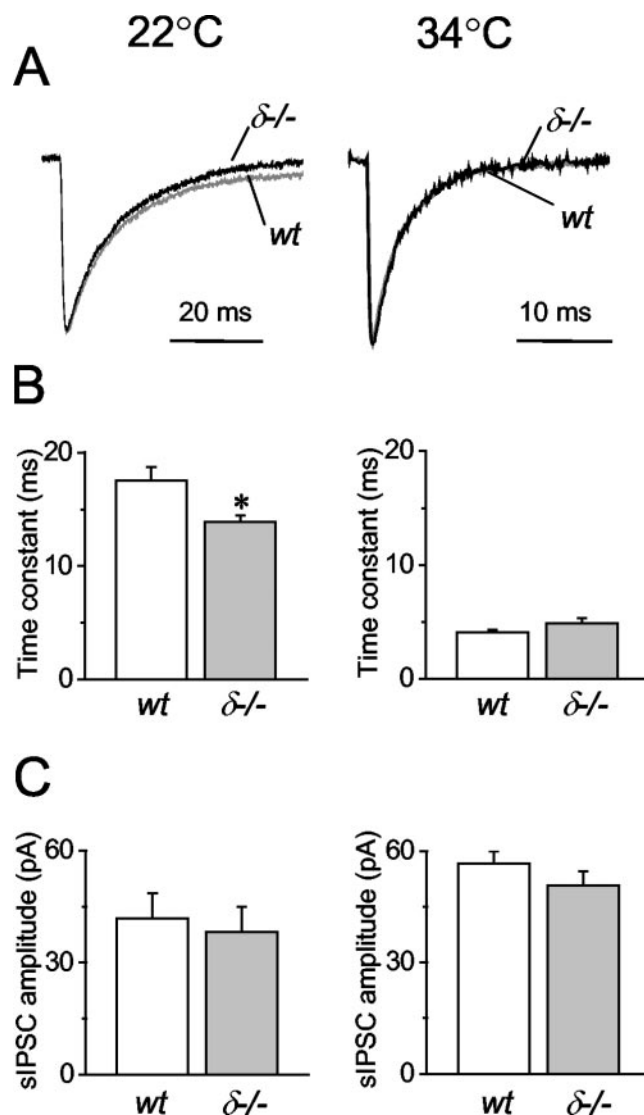
Figure 4. Temperature dependence of sIPSC recorded in wt and δ−/− granule cells. *A*, Normalized and superimposed sIPSC averages from >100 events in wt (gray trace) and in δ−/− (black trace) mice at 22° and 34°C, respectively. *B*, The weighted decay time constants are slower in wt ($n = 10$) than in δ−/− ($n = 9$) mice at 22°C (*$p < 0.01$; t test), whereas they are similar at 34°C (wt, $n = 5$; δ−/−, $n = 6$). *C*, sIPSC amplitudes are also temperature dependent but not significantly different between wt ($n = 10$ at 22°C; $n = 5$ at 34°C) and δ−/− ($n = 9$ at 22°C; $n = 6$ at 34°C) mice.

was not significantly different ($p > 0.05$ two-tailed t test) from the decay time of sIPSCs recorded in granule cells of δ−/− mice (Figs. 4B, 5B).

Effects of Zn^{2+} and the GABA transporter GAT-1 inhibitor NO711 on IPSCs evoked by minimal stimulation at somatic and dendritic sites in wt and δ−/− mice

Stimulating electrodes pulled of Θ−glass can be used effectively to produce minimal stimulation of the granule cells for the study of quantal synaptic transmission (Nusser et al., 1998a). In the present study we used such stimulating electrodes placed near the soma and in the molecular layer to evoke IPSCs by minimal stimulation. On the basis of our light microscopic studies of the distribution of δ subunits in the dentate gyrus (Fig. 1A,B), we tested the possibility that there might be considerable differences between

the activation of such receptors in the somata and the dendrites of granule cells even at near-physiological temperatures.

The weighted decay time constants of minimal eIPSCs evoked by stimulation of GABAergic fibers near the soma were similar between wt and $\delta-/-$ mice (Table 2, Fig. 6A,B). The amplitudes and 10–90% RTs were also comparable in the two genotypes (Table 2). In contrast, eIPSCs elicited by minimal stimulation in the molecular layer of wt mice decayed 75% slower than those in $\delta-/-$ animals ($p < 0.05$; two-tailed t test) (Table 2, Fig. 6A,B). These findings are consistent with a predominantly dendritic localization of the δ subunit-containing GABA_A receptors. The longer decay times of dendritically evoked IPSCs in wt granule cells may stem from the activation of these receptors at the periphery of the inhibitory synapses by GABA spillover after local stimulation. The large number of terminals and corresponding release sites in this layer would favor the overspill-dependent activation of GABA receptors (Overstreet and Westbrook, 2003).

If δ subunit-containing GABA_A receptors contribute to shaping the eIPSCs, the events should be preferentially sensitive to low concentrations of Zn^{2+}. The IC_{50} of Zn^{2+} at these receptors is <16 μM (Saxena and Macdonald, 1996; Krishek et al., 1998; Korpi et al., 2002a). The rationale was to compare the effects of Zn^{2+} in wt and $\delta-/-$ granule cells to eliminate the possibility that Zn^{2+} might have blocked the activation of GABA_A receptors made up of only α and β subunits that are known to have the highest sensitivity to Zn^{2+} (Hosie et al., 2003). Table 3 summarizes the results of paired experiments in which somatic and dendritic stimulations. Perfusion of $ZnCl_2$ (10 μM) had no significant effects ($p = 0.34$; paired t test) on the decay of eIPSCs evoked by stimulation near the somata of granule cells in wt animals, and the eIPSC traces recorded in wt, wt + Zn^{2+}, and $\delta-/-$ granule cells were virtually superimposable (Fig. 6A, top panel). The amplitudes and 10–90% RTs of somatic eIPSCs were similarly unaffected by Zn^{2+} (Table 3). In contrast, Zn^{2+} significantly ($p < 0.05$; paired two-tailed t test) accelerated the decays of eIPSCs elicited by minimal stimulation in the stratum moleculare to approximately two-thirds of control values (Table 3), yielding eIPSCs with very similar time courses in the wt + Zn^{2+}, $\delta-/-$, and $\delta-/- + Zn^{2+}$ experimental conditions (Fig. 6A, bottom panel). The average value of the decay of the dendritically evoked wt eIPSC in the presence of Zn^{2+} is comparable with the pooled average decay of 17.4 msec of the dendritic stimulation eIPSCs in $\delta-/-$ granule cells (Table 2). In wt granule cells, Zn^{2+} decreased the amplitude of eIPSCs elicited by dendritic stimulation by 29% (Table 3) ($p < 0.05$; paired two-tailed t test), whereas the 10–90% RTs remained constant. As depicted in Table 3 and Figure 6B, neither the amplitudes nor the decay time constants of dendritically evoked eIPSCs were altered by Zn^{2+} in $\delta-/-$ granule cells.

Because Zn^{2+} also had an effect only on the decay of sIPSCs recorded in wt granule cells at room temperature where GABA uptake should be impaired, the uptake of GABA may regulate the activation of δ subunit-containing GABA_A receptors by spillover
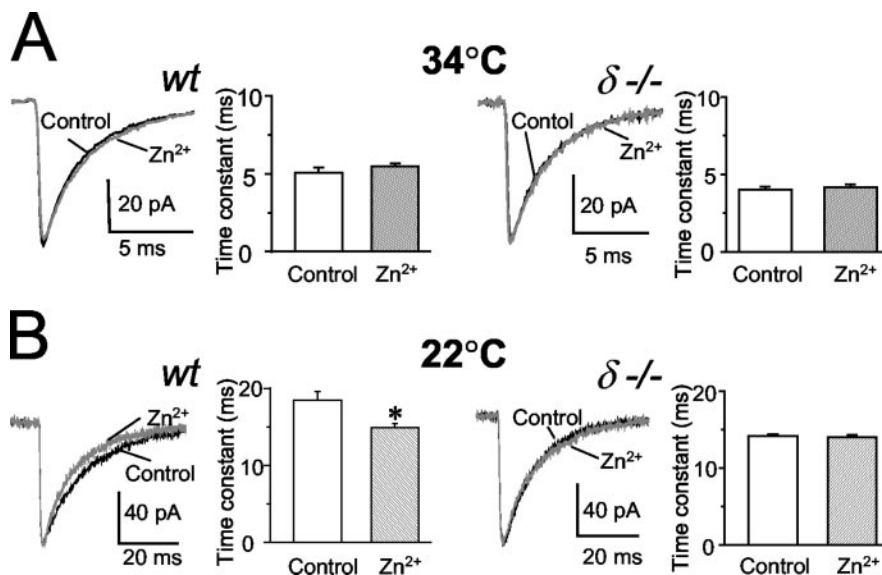
Figure 5. The effect of Zn^{2+} on sIPSC kinetics in wt and $\delta-/-$. A, At 34°C, $ZnCl_2$ (10 μM) had no significant effect on the decay time constants of sIPSCs recorded in either wt ($n = 5$) or $\delta-/-$ ($n = 6$) granule cells. B, At 22°C, perfusion of 10 μM $ZnCl_2$ reduced the weighted sIPSC decay time constant in wt ($n = 7$; *$p < 0.01$; paired two-tailed t test) to a value similar to that found in $\delta-/-$ mice at the same temperature (Fig. 4B). In contrast, 10 μM $ZnCl_2$ does not significantly affect the decay time constants of sIPSCs in $\delta-/-$ neurons ($n = 5$; $p > 0.05$; paired two-tailed t test). Raw traces are averages of 60–120 sIPSCs.

of GABA from the active synapse or from neighboring synapses. Some of the sIPSCs may have originated from proximal dendritic sites (Soltesz et al., 1995), because somatic eIPSCs were found to be insensitive to Zn^{2+} in wt granule cells. To address more specifically the role of GABA uptake in shaping the time course of eIPSCs through the activation of δ subunit-containing GABA_A receptors, we tested the effects of the specific GAT-1 GABA transporter inhibitor NO711 (10 μM) (Borden et al., 1994) on eIPSCs elicited by somatic or dendritic stimulation in wt and $\delta-/-$ mice. Blocking GAT-1 in wt neurons had no significant effect on the amplitudes, 10–90% RTs, and decay kinetics of sIPSCs or of somatically evoked eIPSCs in four cells (Table 4, Fig. 7A,B). In contrast, NO711 significantly prolonged ($p < 0.05$; paired two-tailed t test) by 92% the decays of dendritically evoked eIPSCs in four wt neurons without affecting their amplitude and 10–90% RTs (Table 4). NO711, however, failed to affect any of the characteristics of dendritically evoked eIPSCs recorded in $\delta-/-$ granule cells (Table 4, Fig. 6A,B). These results are consistent with a higher density of δ subunit-containing receptors in the molecular layer of wt animals and their activation by GABA overspill, which is under the strict control of GAT-1-mediated GABA uptake.

Discussion

The main findings of our study are as follows: (1) in granule cells of the mouse dentate gyrus, δ subunit-containing GABA_A receptors are localized predominantly at the edge of symmetric synapses on dendrites in the molecular layer, and (2) at near-physiological temperature, these receptors do not participate in shaping sIPSCs unless GABA overspill occurs when the GAT-1-dependent GABA uptake system is impaired or when large amounts of GABA are released from inhibitory terminals. This very specific localization together with a high Zn^{2+} sensitivity endows these receptors with a special role in regulating the excitability of granule cells.

Table 2. Characteristics of eIPSCs evoked by minimal stimulation in dentate gyrus granule cells of wt and δ−/− mice

	wt		δ−/−	
	Soma	Dendrite	Soma	Dendrite
Amplitude (pA) @V_h = −70 mV	−157.6 ± 21.8	−139.9 ± 15.7	−124.8 ± 26.7	−116.4 ± 17.0
$RT_{10-90\%}$ (msec)	0.95 ± 0.21	2.73 ± 0.40	1.10 ± 0.21	2.99 ± 0.32
τ_w (msec)	7.6 ± 0.4	30.6 ± 1.4	6.6 ± 0.5	17.4 ± 1.3*
Number of cells	11	11	7	16

* denotes a difference with a $p < 0.05$ at the corresponding stimulus locations; two-tailed t test between genotypes.
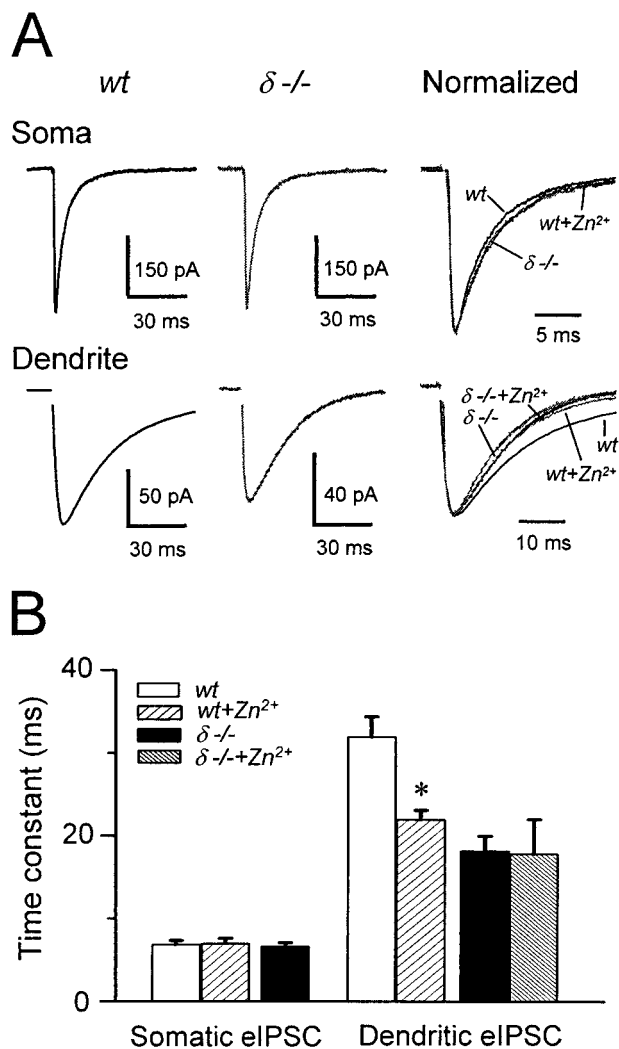
Figure 6. The effect of Zn^{2+} on eIPSCs elicited from somatic and dendritic stimulation sites in wt and δ−/− granule cells. A, Stimulating electrodes positioned near the soma (Soma) and in the molecular layer (Dendrite) were used to elicit eIPSCs by minimal stimulation. Traces are averages of >30 events from wt and δ−/− slices. The rightmost panels show normalized events at expanded time scales to illustrate the effect of 10 μM ZnCl$_2$ (Zn^{2+}) on eIPSCs elicited from both sites in wt and on dendritically evoked events in wt and δ−/− granule cells. B, Summary data for five experiments each. Weighted decay time constants of somatic eIPSCs are comparable between wt and δ−/− granule cells ($p > 0.05$; two-tailed t test), and Zn^{2+} does not affect the decays of somatic eIPSCs in wt neurons ($p > 0.05$; paired two-tailed t test). In contrast, dendritically evoked eIPSCs in wt granule cells decay significantly faster in the presence of ZnCl$_2$ (10 μM) than under control conditions (*$p < 0.01$; paired two-tailed t test). The dendritically evoked eIPSCs of δ−/− mice decay significantly faster than those recorded in wt granule cells (Table 2) and are unaffected by Zn^{2+} ($p > 0.05$; paired two-tailed t test).

Dendritic localization of δ subunit-containing GABA$_A$ receptors

At the light microscopic level, we found dense δ subunit labeling in the molecular layer, with substantially less staining in the gran-

ule cell layer and hilar region. This is similar to the distribution seen in the rat (Fritschy and Möhler, 1995; Sperk et al., 1997) and that described previously in the mouse (Peng et al., 2002). It is not known whether the light staining in the granule cell layer reflects a genuine low level of the subunits on the somata of granule cells or whether it represents the distribution of the receptor on granule cell dendrites that are situated in this layer. Only one-fourth of the total number of inhibitory synapses is found on granule cell somata or axon initial segments in the granule cell layer (Halasy and Somogyi, 1993a). The bulk (75%) of inhibitory synapses is found in the molecular layer and originates from several well defined inhibitory neuron types (Halasy and Somogyi, 1993b; Han et al., 1993). The predominance of δ subunit-containing GABA$_A$ receptors in the molecular layer makes it likely that their activation will depend on GABA released from these specific interneurons, although at this time we cannot ascertain whether all or just some of the four to five different interneuron types will activate these receptors. Considering the mutually exclusive dendritic domains of granule cells innervated by these specific cells (Han et al., 1993) and the homogeneous δ subunit-IR staining in the molecular layer, however, it is possible that each type of dendritically projecting interneuron is able to activate δ subunit-containing receptors.

Our electrophysiological recordings and minimal local stimulation experiments are consistent with the dendritic localization of δ subunit-containing GABA$_A$ receptors. Minimal stimulation in the molecular but not in the granule cell layer elicited eIPSCs that were selectively reduced by low concentrations of Zn^{2+} and were enhanced by the GAT-1 blocker NO711. The GABA uptake blocker has been shown to produce a robust prolongation of IPSCs evoked by focal stimulation in the granule cell layer of postnatal day 13–15 rat slices at 33°C (Overstreet and Westbrook, 2003). The lack of effect of NO711 in our recordings of eIPSCs with fast kinetics elicited by somatic stimulation may be attributable to specific activation of predominantly basket cell terminals. The lower release site density may make these synapses less prone to overspill, and thus they would be less affected by GABA uptake blockers (Overstreet and Westbrook, 2003). In contrast, the kinetics of eIPSCs evoked by stimulation in the molecular layer were slow, most likely because of cable distortion of inhibitory currents produced on electrotonically remote dendrites, as shown for CA1 pyramidal neurons (Maccaferri et al., 2000). Because dentate granule cells are considerably more electrotonically compact than CA1 pyramidal cells (Carnevale et al., 1997), however, there are two other possible explanations: (1) slow eIPSCs elicited by molecular layer stimulation in our experiments have a different "at source" kinetics because of different GABA$_A$ receptor assemblies at dendritic synapses, or (2) perisynaptic receptors are activated by GABA overspill. We favor the latter explanation because the reduced amplitude and decay of dendritically elicited eIPSCs by low concentrations of Zn^{2+} are consistent with Zn^{2+}-sensitive δ subunit-containing receptors activated during eIPSCs.

In line with the lack of differences in somatically elicited

Table 3. The effect of Zn^{2+} on eIPSCs evoked by minimal stimulation in dentate gyrus granule cells of wt and δ −/− mice

	wt		wt + Zn^{2+}		δ−/−	δ−/− + Zn^{2+}
	Soma	Dendrite	Soma	Dendrite	Dendrite	Dendrite
Amplitude (pA) @V_h = −70 mV	−119.8 ± 26.4	−157.3 ± 16.0	−106.2 ± 23.5	−85.8 ± 9.3*	−104.1 ± 17.9	−111.5 ± 13.0
RT$_{10-90\%}$ (msec)	1.35 ± 0.40	2.98 ± 0.79	1.06 ± 0.21	3.40 ± 0.66	2.62 ± 0.65	2.90 ± 0.70
τ_w (msec)	8.2 ± 1.0	32.5 ± 1.1	7.0 ± 0.6	22.0 ± 1.1*	17.8 ± 3.8	17.8 ± 4.1
Number of cells	5	5	5	5	5	5

* denotes $p < 0.05$, paired two tailed t test, between corresponding stimulation sites under control conditions and in the presence of 10 μM ZnCl$_2$.

Table 4. The effect of the GAT-1 antagonist NO711 on eIPSCs evoked by minimal stimulation and sIPSCs in dentate gyrus granule cells of wt and δ−/− mice

|	wt		wt + NO711		δ−/−	δ−/− + NO711
	Soma	Dendrite	Soma	Dendrite	Dendrite	Dendrite
eIPSCs						
Amplitude (pA) @V_h = −70 mV	−180.5 ± 44.1	−135.5 ± 32.7	−205.2 ± 47.8	−162.8 ± 39.8	−125.5 ± 7.7	−110.5 ± 4.7
RT$_{10-90\%}$ (msec)	0.49 ± 0.05	2.00 ± 0.35	0.44 ± 0.03	1.87 ± 0.33	3.87 ± 0.33	3.99 ± 0.35
τ_w (msec)	7.6 ± 0.4	28.3 ± 3.4	8.2 ± 0.5	54.3 ± 7.5*	16.3 ± 2.1	18.7 ± 1.7
sIPSCs						
Frequency (H$_2$)	7.5 ± 2.0		6.7 ± 2.0		5.4 ± 0.7	6.1 ± 1.1
Amplitude @V_h = −70 mV	−48.7 ± 5.2		−51.6 ± 5.3		−43.5 ± 3.6	−41.7 ± 2.4
RT$_{10-90\%}$ (msec)	0.326 ± 0.02		0.358 ± 0.01		0.308 ± 0.01	0.332 ± 0.005
τ_w (msec)	4.97 ± 0.62		5.74 ± 0.64		4.17 ± 0.29	4.16 ± 0.18
Number of cells	4	4	4	4	4	4

* denotes $p < 0.05$, paired two-tailed t test, between corresponding stimulation sites under control conditions and in the presence of 10 μM NO711.

eIPSCs between wt and δ−/− granule cells, we found no differences in the kinetics of sIPSCs recorded in the two preparations. This is to be expected if most of the spontaneous activity recorded in dentate gyrus granule cells originates from somatic or proximal dendritic synapses (Soltesz et al., 1995), where δ subunit-containing receptors are scarce; however, our finding is at odds with previously published studies in dentate granule cells of δ−/− animals describing a significantly faster decay of mIPSCs in the absence of δ subunits (Mihalek et al., 1999; Spigelman et al., 2002). The discrepancy may stem from the lower recording temperature in those studies resulting in a diminished GABA uptake. Our results are consistent with this possibility because we also found significantly faster decaying average sIPSCs in δ−/− granule cells at room temperature when GABA uptake is vastly reduced (Mitchell and Silver, 2000). Interestingly, a recent study (Porcello et al., 2003) reported no difference between wt and δ−/−preparations in the decay time constants of sIPSCs recorded at room temperature in another δ subunit-rich area, the thalamic relay nuclei. This may mean that thalamic δ subunits might be located farther away from inhibitory synapses, i.e., they are truly extrasynaptically as in cerebellar granule cells (Nusser et al., 1998b), or that GABA uptake processes are much stronger in the thalamus than in the dentate gyrus.

Perisynaptic localization

At the ultrastructural level, δ subunit-containing GABA$_A$ receptors were found to be localized perisynaptically, at the edge of GABA synapses on dendrites, whereas the α2 subunits were situated within the boundaries of inhibitory synapses. These distinct labeling patterns presumably identified sites with the highest densities of each subunit. Because of the reduced sensitivity of many postembedding immunogold methods (Somogyi et al., 1996), the current findings do not preclude the presence of either subunit at additional synaptic and extrasynaptic locations, presumably at lower densities. The different labeling patterns, however, obtained with very similar postembedding methods in tissue from the same animals, strongly suggest that the δ and α2
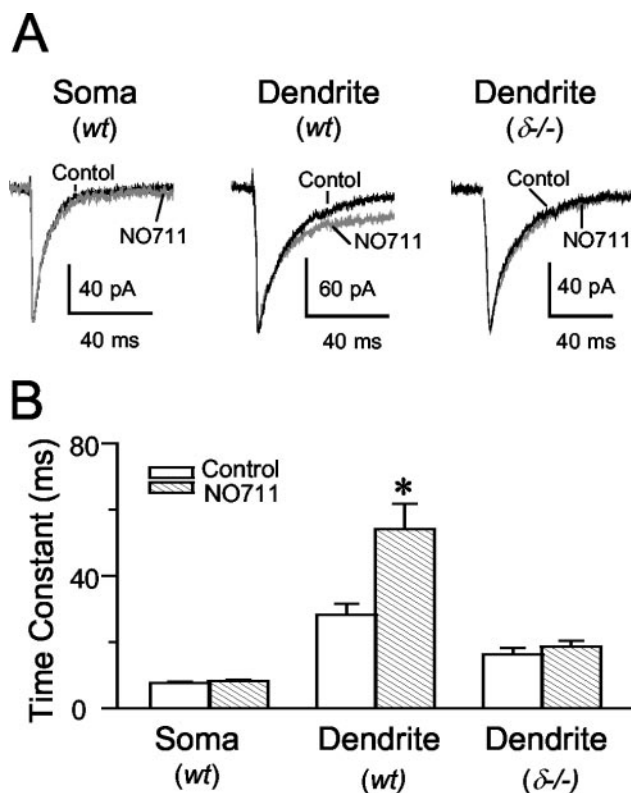
Figure 7. Effect of the GAT-1 GABA transporter inhibitor NO711 (10 μM) on somatically and dendritically elicited eIPSCs in wt and δ−/− granule cells. A, Averaged somatic (Soma) eIPSCs in wt and dendritic (Dendrite) eIPSCs in δ−/− (>30 each) recorded at 34°C are not affected by NO711. Only the dendritic eIPSCs of the wt are prolonged by the uptake blocker. B, Summary of weighted decay time constants of eIPSCs in four experiments each. Perfusion of 10 μM NO711 had no effect on the decays of somatic eIPSCs of wt or on the decays of dendritic eIPSCs in δ−/− granule cells ($p > 0.05$; paired two-tailed t test). In contrast, NO711 further prolonged (191% of pre-drug control) the already long, weighted decay time constants of dendritic eIPSCs of wt granule cells (*$p < 0.01$; paired two-tailed t test).

subunits are concentrated most highly at perisynaptic and synaptic locations, respectively.

The absence of δ subunit-containing GABA_A receptors directly at the postsynaptic densities of symmetric synapses on granule cells is reminiscent of the findings in cerebellar granule cells where these receptors are also found outside the synapse (Nusser et al., 1998b). The difference between the distributions of these receptors in the two cell types is the predominantly perisynaptic localization of the δ subunits in dentate granule cells compared with the clear extrasynaptic localization of the receptors in cerebellar neurons (Nusser et al., 1998b). This perisynaptic arrangement makes it more likely for the δ subunit-containing receptors of dentate gyrus granule cells to be activated by phasic GABA release coincident with the activation of synaptic receptors; however, our electrophysiological findings indicate that phasic, action potential-dependent GABA release is not likely to activate these receptors unless certain conditions are satisfied.

These conditions are met during stimulus-evoked GABA release or probably under high-frequency firing of the dendritically synapsing interneurons. Evoked release of GABA can cause considerable overspill of transmitter to extrasynaptic receptors (Roepstorff and Lambert, 1994), a process regulated by GABA uptake in both hippocampal (Roepstorff and Lambert, 1994) and cerebellar neurons (Mitchell and Silver, 2000). Our findings show that GABA released by minimal stimulation in the dendritic layer, where most of the δ subunit-containing receptors are located, can activate the perisynaptic receptors, thus prolonging the decay of synaptic currents. It remains to be determined under what circumstances there is adequate activation of GABAergic terminals synapsing onto granule cell dendrites to release sufficient GABA to spill over to the perisynaptic receptors.

Physiological and pharmacological consequences

The selective dendritic distribution of δ subunit-containing GABA_A receptors puts them in a special position for the regulation of neuronal excitability. Depending on the compound equilibrium potential of the ions permeating through GABA_A receptor channels, dendritic IPSPs may become effectively excitatory by the time they passively propagate to the soma (Gulledge and Stuart, 2003). Indeed, using noninvasive techniques in dentate gyrus granule cells, the GABA reversal potential has been measured to be ~15 mV depolarized from rest (Soltesz and Mody, 1994). Consequently, when dendritic δ subunit-containing GABA_A receptors are activated by overspill resulting in the prolongation of the GABA conductance, a much more prolonged depolarization would be transmitted to the soma that may serve as a boost for other excitatory events. At the same time, a prolonged local shunting inhibition (Staley and Mody, 1992) may dampen excitatory inputs arriving at dendritic sites. If these perisynaptic GABA_A receptors are continually exposed to ambient levels of GABA, they may indeed be responsible for the tonic current observed in dentate gyrus granule cells (Nusser and Mody, 2002; Stell and Mody, 2002).

Perisynaptically localized δ subunit-containing GABA_A receptors also have several interesting pharmacological consequences. If indeed α4βδ subunit combinations are found around inhibitory synapses in wt animals, such receptors would be particularly insensitive to BZ. First, the presence of the α4 subunit renders receptors insensitive to conventional BZ (Korpi et al., 2002a), and second, the δ subunit-containing receptors most likely exclude γ subunits, which is a requirement for BZ sensitivity (Günther et al., 1995; Smith and Olsen, 1995). Therefore, currents through δ subunit–containing receptors activated by

GABA overspill should not be affected by BZ. In contrast, GAT-1 inhibitors may be especially useful in enhancing this type of receptor activation as shown by specific enhancement of tonic inhibition (Nusser and Mody, 2002; Stell and Mody, 2002).

Although the modulation by benzodiazepines and GAT-1 blockers may be purely of pharmacologic or therapeutic significance, endogenous modulators such as Zn^{2+} and neurosteroids may have selective effects on perisynaptic δ subunit-containing receptors. The elevated Zn^{2+} sensitivity of γ subunit-lacking (Draguhn et al., 1990; Smart et al., 1991) but δ subunit-containing receptors (Korpi et al., 2002a), also shown in our study, may make these receptors especially vulnerable to inhibition by ambient levels of Zn^{2+}. It is interesting to note that the IC_{50} for Zn^{2+} inhibition of α4β3δ and α4β3γ2 GABA_A receptors was found to be similar (~2 μM) in receptors expressed by a stable fibroblast cell line (Brown et al., 2002). Therefore, the lack of sensitivity to Zn^{2+} of sIPSCs and eIPSCs in δ−/− granule cells may indicate that the compensatory upregulation of γ2 subunits in δ−/− mice (Tretter et al., 2001; Korpi et al., 2002b; Peng et al., 2002) does not yield combinations with α4 subunits. Considering the equal Zn^{2+} sensitivity of α4β3δ and α4β3γ2 GABA_A receptors (Brown et al., 2002) and the reduced levels of α4 subunits in these mice (Peng et al., 2002), the lack of a Zn^{2+}-sensitive overspill component may be caused by the loss of α4β3γ2 receptors from perisynaptic sites. This possibility appears to be highly unlikely in light of the predominant synaptic localization of γ2 subunits (Somogyi et al., 1996; Essrich et al., 1998) and our present findings demonstrating the perisynaptic localization of δ subunit-containing GABA_A receptors. Alternatively, the Zn^{2+} sensitivity of native neuronal α4β3γ2 receptors may be much lower than that seen for receptors expressed in fibroblasts.

Zinc can be released during heightened neuronal activity from Zn^{2+}-containing terminals that include the perforant pathway (Frederickson, 1989). Even if the vesicular Zn^{2+} released after stimulation is too low to have an effect on most ligand- or voltage-gated ion channels, there appears to be a "Zn^{2+} veneer" made up of Zn^{2+} loosely bound to various extracellular elements (Kay, 2003). This pool of Zn^{2+} is sufficiently large to create a local concentration reaching a few micromolar (Kay, 2003) that may affect the δ subunit-containing GABA_A receptors Accordingly, the δ subunit-containing receptors may be under the control of vesicular Zn^{2+} released from the excitatory terminals or the Zn^{2+} veneer even under normal physiological conditions. This is in sharp contrast to the synaptic GABA_A receptors that become sensitive to much higher concentrations of Zn^{2+} and only in temporal lobe epilepsy (Buhl et al., 1996; Brooks-Kayal et al., 1998; Cohen et al., 2003) when sufficient amounts of the cation can be released from the sprouted mossy fibers. In addition to Zn^{2+}, neurosteroids may be the other endogenous modulator of the δ subunit-containing GABA_A receptors. Recent findings have shown the high sensitivity of these receptors to neuroactive steroids (Brown et al., 2002; Wohlfarth et al., 2002) that enhance the efficacy of GABA by several-fold. Neurosteroids would thus produce much larger currents during activation of perisynaptic δ subunit-containing receptors, triggering profound consequences on cellular excitability in the dentate gyrus.

The precise details of the activation and modulation of δ subunit-containing GABA_A receptors of dentate gyrus granule cells remain to be determined. Nevertheless, it is clear that their specific localization around dendritic GABA synapses endows them with unique roles in controlling the transmission of neuronal impulses through the gateway to the hippocampal formation.

References

Borden LA, Murali Dhar TG, Smith KE, Weinshank RL, Branchek TA, Gluchowski C (1994) Tiagabine, SK&F 89976-A, CI-966, and NNC-711 are selective for the cloned GABA transporter GAT-1. Eur J Pharmacol 269:219–224.

Brickley SG, Cull-Candy SG, Farrant M (1996) Development of a tonic form of synaptic inhibition in rat cerebellar granule cells resulting from persistent activation of GABA_A receptors. J Physiol (Lond) 497:753–759.

Brickley SG, Revilla V, Cull-Candy SG, Wisden W, Farrant M (2001) Adaptive regulation of neuronal excitability by a voltage-independent potassium conductance. Nature 409:88–92.

Brooks-Kayal AR, Shumate MD, Jin H, Rikhter TY, Coulter DA (1998) Selective changes in single cell GABA_A receptor subunit expression and function in temporal lobe epilepsy. Nat Med 4:1166–1172.

Brown N, Kerby J, Bonnert TP, Whiting PJ, Wafford KA (2002) Pharmacological characterization of a novel cell line expressing human α4β3δ GABA_A receptors. Br J Pharmacol 136:965–974.

Buhl EH, Otis TS, Mody I (1996) Zinc-induced collapse of augmented inhibition by GABA in a temporal lobe epilepsy model. Science 271:369–373.

Carnevale NT, Tsai KY, Claiborne BJ, Brown TH (1997) Comparative electrotonic analysis of three classes of rat hippocampal neurons. J Neurophysiol 78:703–720.

Cohen AS, Lin DD, Quirk GL, Coulter DA (2003) Dentate granule cell GABA_A receptors in epileptic hippocampus: enhanced synaptic efficacy and altered pharmacology. Eur J Neurosci 17:1607–1616.

Draguhn A, Verdorn TA, Ewert M, Seeburg PH, Sakmann B (1990) Functional and molecular distinction between recombinant rat GABAA receptor subtypes by Zn²⁺. Neuron 5:781–788.

Essrich C, Lorez M, Benson JA, Fritschy JM, Luscher B (1998) Postsynaptic clustering of major GABAA receptor subtypes requires the gamma 2 subunit and gephyrin. Nat Neurosci 1:563–571.

Frederickson CJ (1989) Neurobiology of zinc and zinc-containing neurons. Int Rev Neurobiol 31:145–238.

Fritschy JM, Möhler H (1995) GABA_A-receptor heterogeneity in the adult rat brain: differential regional and cellular distribution of seven major subunits. J Comp Neurol 359:154–194.

Gulledge AT, Stuart GJ (2003) Excitatory actions of GABA in the cortex. Neuron 37:299–309.

Günther U, Benson J, Benke D, Fritschy JM, Reyes G, Knoflach F, Crestani F, Aguzzi A, Arigoni M, Lang Y, Bluethmann H, Möhler H, Lüscher B (1995) Benzodiazepine-insensitive mice generated by targeted disruption of the gamma 2 subunit gene of gamma-aminobutyric acid type A receptors. Proc Natl Acad Sci USA 92:7749–7753.

Haas KF, Macdonald RL (1999) GABA_A receptor subunit gamma2 and delta subtypes confer unique kinetic properties on recombinant GABA_A receptor currents in mouse fibroblasts. J Physiol (Lond) 514:27–45.

Halasy K, Somogyi P (1993a) Distribution of GABAergic synapses and their targets in the dentate gyrus of rat: a quantitative immunoelectron microscopic analysis. J Hirnforsch 34:299–308.

Halasy K, Somogyi P (1993b) Subdivisions in the multiple GABAergic innervation of granule cells in the dentate gyrus of the rat hippocampus. Eur J Neurosci 5:411–429.

Hamann M, Rossi DJ, Attwell D (2002) Tonic and spillover inhibition of granule cells control information flow through cerebellar cortex. Neuron 33:625–633.

Han ZS, Buhl EH, Lorinczi Z, Somogyi P (1993) A high degree of spatial selectivity in the axonal and dendritic domains of physiologically identified local-circuit neurons in the dentate gyrus of the rat hippocampus. Eur J Neurosci 5:395–410.

Hosie AM, Dunne EL, Harvey RJ, Smart TG (2003) Zinc-mediated inhibition of GABA_A receptors: discrete binding sites underlie subtype specificity. Nat Neurosci 6:362–369.

Jechlinger M, Pelz R, Tretter V, Klausberger T, Sieghart W (1998) Subunit composition and quantitative importance of hetero-oligomeric receptors: GABA_A receptors containing α6 subunits. J Neurosci 18:2449–2457.

Jiao Y, Sun Z, Lee T, Fusco FR, Kimble TD, Meade CA, Cuthbertson S, Reiner A (1999) A simple and sensitive antigen retrieval method for free-floating and slide-mounted tissue sections. J Neurosci Methods 93:149–162.

Jones A, Korpi ER, McKernan RM, Pelz R, Nusser Z, Mäkelä R, Mellor JR, Pollard S, Bahn S, Stephenson FA, Randall AD, Sieghart W, Somogyi P,

Smith AJH, Wisden W (1997) Ligand-gated ion channel subunit partnerships: GABA_A receptor α_6 subunit gene inactivation inhibits δ subunit expression. J Neurosci 17:1350–1362.

Kay AR (2003) Evidence for chelatable zinc in the extracellular space of the hippocampus, but little evidence for synaptic release of Zn. J Neurosci 23:6847–6855.

Korpi ER, Grunder G, Lüddens H (2002a) Drug interactions at GABA_A receptors. Prog Neurobiol 67:113–159.

Korpi ER, Mihalek RM, Sinkkonen ST, Hauer B, Hevers W, Homanics GE, Sieghart W, Lüddens H (2002b) Altered receptor subtypes in the forebrain of GABA_A receptor delta subunit-deficient mice: recruitment of gamma 2 subunits. Neuroscience 109:733–743.

Krishek BJ, Moss SJ, Smart TG (1998) Interaction of H⁺ and Zn²⁺ on recombinant and native rat neuronal GABAA receptors. J Physiol (Lond) 507:639–652.

Maccaferri G, Roberts JD, Szucs P, Cottingham CA, Somogyi P (2000) Cell surface domain specific postsynaptic currents evoked by identified GABAergic neurones in rat hippocampus in vitro. J Physiol (Lond) 1:91–116.

Marksitzer R, Benke D, Fritschy JM, Trzeciak A, Bannwarth W, Möhler H (1993) GABAA-receptors: drug binding profile and distribution of receptors containing the alpha 2-subunit in situ. J Recept Res 13:467–477.

Matsubara A, Laake JH, Davanger S, Usami S, Ottersen OP (1996) Organization of AMPA receptor subunits at a glutamate synapse: a quantitative immunogold analysis of hair cell synapses in the rat organ of Corti. J Neurosci 16:4457–4467.

McKernan RM, Whiting PJ (1996) Which GABA_A-receptor subtypes really occur in the brain? Trends Neurosci 19:139–143.

Mellor JR, Randall AD (1998) Voltage-dependent deactivation and desensitization of GABA responses in cultured murine cerebellar granule cells. J Physiol (Lond) 506:377–390.

Mihalek RM, Banerjee PK, Korpi ER, Quinlan JJ, Firestone LL, Mi ZP, Lagenaur C, Tretter V, Sieghart W, Anagnostaras SG, Sage JR, Fanselow MS, Guidotti A, Spigelman I, Li Z, DeLorey TM, Olsen RW, Homanics GE (1999) Attenuated sensitivity to neuroactive steroids in gamma-aminobutyrate type A receptor delta subunit knockout mice. Proc Natl Acad Sci USA 96:12905–12910.

Mitchell SJ, Silver RA (2000) GABA spillover from single inhibitory axons suppresses low-frequency excitatory transmission at the cerebellar glomerulus. J Neurosci 20:8651–8658.

Mody I (2001) Distinguishing between GABA_A receptors responsible for tonic and phasic conductances. Neurochem Res 26:907–913.

Nusser Z, Mody I (2002) Selective modulation of tonic and phasic inhibitions in dentate gyrus granule cells. J Neurophysiol 87:2624–2628.

Nusser Z, Sieghart W, Benke D, Fritschy JM, Somogyi P (1996) Differential synaptic localization of two major gamma-aminobutyric acid type A receptor α subunits on hippocampal pyramidal cells. Proc Natl Acad Sci USA 93:11939–11944.

Nusser Z, Hájos N, Somogyi P, Mody I (1998a) Increased number of synaptic GABA_A receptors underlies potentiation at hippocampal inhibitory synapses. Nature 395:172–177.

Nusser Z, Sieghart W, Somogyi P (1998b) Segregation of different GABA_A receptors to synaptic and extrasynaptic membranes of cerebellar granule cells. J Neurosci 18:1693–1703.

Nusser Z, Naylor D, Mody I (2001) Synapse-specific contribution of the variation of transmitter concentration to the decay of inhibitory postsynaptic currents. Biophys J 80:1251–1261.

Otis TS, Mody I (1992) Modulation of decay kinetics and frequency of GABA_A receptor-mediated spontaneous inhibitory postsynaptic currents in hippocampal neurons. Neuroscience 49:13–32.

Overstreet LS, Westbrook GL (2003) Synapse density regulates independence at unitary inhibitory synapses. J Neurosci 23:2618–2626.

Peng Z, Hauer B, Mihalek RM, Homanics GE, Sieghart W, Olsen RW, Houser CR (2002) GABA_A receptor changes in delta subunit-deficient mice: altered expression of alpha4 and gamma2 subunits in the forebrain. J Comp Neurol 446:179–197.

Pirker S, Schwarzer C, Wieselthaler A, Sieghart W, Sperk G (2000) GABA_A receptors: immunocytochemical distribution of 13 subunits in the adult rat brain. Neuroscience 101:815–850.

Pitler TA, Alger BE (1994) Depolarization-induced suppression of GABAergic inhibition in rat hippocampal pyramidal cells: G protein involvement in a presynaptic mechanism. Neuron 13:1447–1455.

Porcello DM, Huntsman MM, Mihalek RM, Homanics GE, Huguenard JR (2003) Intact synaptic GABAergic inhibition and altered neurosteroid modulation of thalamic relay neurons in mice lacking delta subunit. J Neurophysiol 89:1378–1386.

Roepstorff A, Lambert JDC (1994) Factors contributing to the decay of the stimulus-evoked IPSC in rat hippocampal CA1 neurons. J Neurophysiol 72:2911–2926.

Saxena NC, Macdonald RL (1994) Assembly of GABA_A receptor subunits: role of the δ subunit. J Neurosci 14:7077–7086.

Saxena NC, Macdonald RL (1996) Properties of putative cerebellar gamma-aminobutyric acid_A receptor isoforms. Mol Pharmacol 49:567–579.

Shu SY, Ju G, Fan LZ (1988) The glucose oxidase-DAB-nickel method in peroxidase histochemistry of the nervous system. Neurosci Lett 85:169–171.

Smart TG, Moss SJ, Xie X, Huganir RL (1991) GABAA receptors are differentially sensitive to zinc: dependence on subunit composition. Br J Pharmacol 103:1837–1839.

Smith GB, Olsen RW (1995) Functional domains of GABA_A receptors. Trends Pharmacol Sci 16:162–168.

Soltesz I, Mody I (1994) Patch-clamp recordings reveal powerful GABAergic inhibition in dentate hilar neurons. J Neurosci 14:2365–2376.

Soltesz I, Smetters DK, Mody I (1995) Tonic inhibition originates from synapses close to the soma. Neuron 14:1273–1283.

Somogyi P, Fritschy JM, Benke D, Roberts JDB, Sieghart W (1996) The gamma2 subunit of the GABA_A receptor is concentrated in synaptic junctions containing the α1 and β2/3 subunits in hippocampus, cerebellum and globus pallidus. Neuropharmacology 35:1425–1444.

Sperk G, Schwarzer C, Tsunashima K, Fuchs K, Sieghart W (1997) GABA_A receptor subunits in the rat hippocampus. 1. Immunocytochemical distribution of 13 subunits. Neuroscience 80:987–1000.

Spigelman I, Li Z, Banerjee PK, Mihalek RM, Homanics GE, Olsen RW (2002) Behavior and physiology of mice lacking the GABAA-receptor delta subunit. Epilepsia 43 [Suppl 5]:3–8.

Staley KJ, Mody I (1992) Shunting of excitatory input to dentate gyrus granule cells by a depolarizing GABA_A receptor-mediated postsynaptic conductance. J Neurophysiol 68:197–212.

Stell BM, Mody I (2002) Receptors with different affinities mediate phasic and tonic GABA_A conductances in hippocampal neurons. J Neurosci 22:RC223(1–5).

Sur C, Farrar SJ, Kerby J, Whiting PJ, Atack JR, McKernan RM (1999) Preferential coassembly of alpha4 and delta subunits of the gamma-aminobutyric acidA receptor in rat thalamus. Mol Pharmacol 56:110–115.

Tretter V, Hauer B, Nusser Z, Mihalek RM, Hoger H, Homanics GE, Somogyi P, Sieghart W (2001) Targeted disruption of the GABA_A receptor delta subunit gene leads to an up-regulation of gamma 2 subunit-containing receptors in cerebellar granule cells. J Biol Chem 276:10532–10538.

Wadiche JI, Kavanaugh MP (1998) Macroscopic and microscopic properties of a cloned glutamate transporter/chloride channel. J Neurosci 18:7650–7661.

Wei W, Mody I, Zhang N, Peng Z, Houser CR (2002) Overspill dependent activation and anatomical localization of δ subunit containing GABA_A receptors in the mouse dentate gyrus. Soc Neurosci Abstr 28:148.6.

Wilson RI, Nicoll RA (2001) Endogenous cannabinoids mediate retrograde signaling at hippocampal synapses. Nature 410:588–592.

Wisden W, Laurie DJ, Monyer H, Seeburg PH (1992) The distribution of 13 GABA_A receptor subunit mRNAs in the rat brain. I. Telencephalon, diencephalon, mesencephalon. J Neurosci 12:1040–1062.

Wohlfarth KM, Bianchi MT, Macdonald RL (2002) Enhanced neurosteroid potentiation of ternary GABA_A receptors containing the δ subunit. J Neurosci 22:1541–1549.